NASA Technical Memorandum 104798

Partial Gravity Simulation Using a Pneumatic Actuator with Closed Loop Mechanical Amplification

David M. Ray

JUNE 1994

NASA Technical Memorandum 104798

Partial Gravity Simulation Using a Pneumatic Actuator with Closed Loop Mechanical Amplification

David M. Ray
Lyndon B. Johnson Space Center
Houston, Texas

National Aeronautics and
Space Administration

This publication is available from the NASA Center for AeroSpace Information,
800 Elkridge Landing Road, Linthicum Heights, MD 21090-2934
(301) 621-0390.

Abstract

To support future manned missions to the surface of the Moon and Mars or missions requiring manipulation of payloads and locomotion in space, a training device is required to simulate the conditions of both partial and microgravity as compared to the gravity on Earth. The focus of this paper is to present the development, construction, and testing of a partial gravity simulator which uses a pneumatic actuator with closed loop mechanical amplification.

Results of the testing show that this type of simulator maintains a constant partial gravity simulation with a variation of the simulated body force between 2.2% and 10%, depending on the type of locomotion inputs. The data collected using the simulator show that mean stride frequencies at running speeds at lunar and martian gravity levels are 12% less than those at Earth gravity. The data also show that foot/ground reaction forces at lunar and martian gravity are, respectively, 62% and 51% less than those on Earth.

Contents

Tables

Figures

1.0 Introduction

There are various methods by which partial gravity can be simulated in a one-g Earth environment. Ideally, the simulator will maintain the proper response and motion cues by allowing for unlimited degrees-of-freedom while keeping the subject isolated from any external friction forces generated by the simulator and its associated ground support equipment. The partial gravity simulator under development at the NASA Johnson Space Center (JSC) that is presented in this paper uses a pneumatic actuator with closed loop mechanical amplification. Pogo is the common term for the partial gravity simulator that employs this method; this is the term that will be used throughout this paper. The purpose of the paper is to provide details of the mechanical control and operation of the Pogo vertical servo unit and to present the results of walking and running data collected at reduced gravity levels.

The Pogo system is a combination of hardware salvaged from the partial gravity simulator used during the Apollo Program and additions and upgrades made during current system development and testing. Pogo consists of three major systems: the vertical servo system, the display and control system, and the gimbal support system. The vertical servo system, which is shown in Figure 1(a), provides control of the pneumatic actuator by using servovalve amplifiers.

The vertical servo system and the gimbal support system and their principles of operation will be described before presenting the experimental activities performed on Pogo. The objectives of these activities include the following: to determine the pressure and flow characteristics of the Pogo vertical servo, to test the Pogo response to human locomotion inputs, to determine the error in maintaining partial gravity simulation, and to compare biomechanic data collected on Pogo to results from other partial gravity simulation

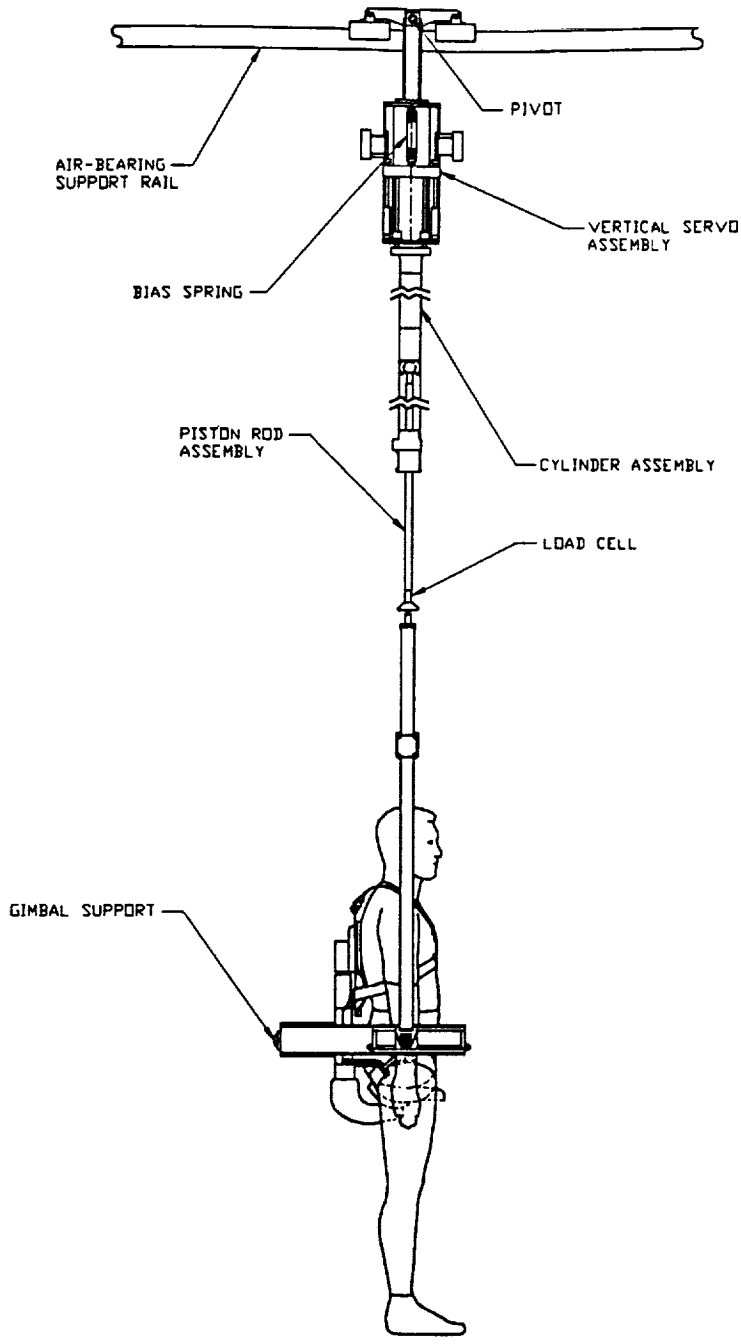

Figure 1(a). Pogo overall configuration.

(Adapted from Trader and Johnson [1] and upgraded by Ray [2]. Gimbal support adapted from NASA drawing SEY43116721, drawn by Brian Petty of the Johnson Engineering Corporation.)

methods. The biomechanic data include mean stride frequency versus gravity level and mean peak foot reaction force versus gravity level.

2.0 Vertical Servo System Description

The vertical servo system is the mechanism on Pogo which applies a constant lifting force opposite to the direction of the Earth's gravity vector. The vertical servo system consists of the vertical servo assembly, the cylinder assembly, and the piston rod assembly, as shown in Figure 1(a). Lifting force is provided by supplying the cylinder with pressurized air which is regulated by the vertical servo assembly. The current available air supply to the vertical servo assembly has a maximum pressure of 120 psig (134.7 psia) and a maximum flow rate of 367 scfm, which is found at standard laboratory conditions of 14.7 psia and 75°F (535°R).

2.1 Gimbal Support System

The gimbal support assembly is the structure a subject is placed on to provide the rotational degrees-of-freedom of pitch, roll, and yaw. Figure 1(b) shows three views of a subject in the gimbal support which is used for shirt-sleeve training exercises. The gimbal support assembly of Figure 1(b) is constructed of aluminum for the structural members and either nylon or kevlar webbing for the support straps. Kevlar is used for the main support straps because of its excellent strength-to-weight ratio and because it does not deflect as much as nylon under loaded conditions. Minimal deflection is important since any forces stored in the straps, due to their elastic properties while deflecting under loaded conditions, will adversely affect the partial gravity simulation. Once a subject is placed on the seat support and strapped into the chest harness, adjustments are made to get the subject's center of gravity to coincide with the pitch and roll axes of the gimbal. A full 360° rotational freedom is capable about the yaw axis.

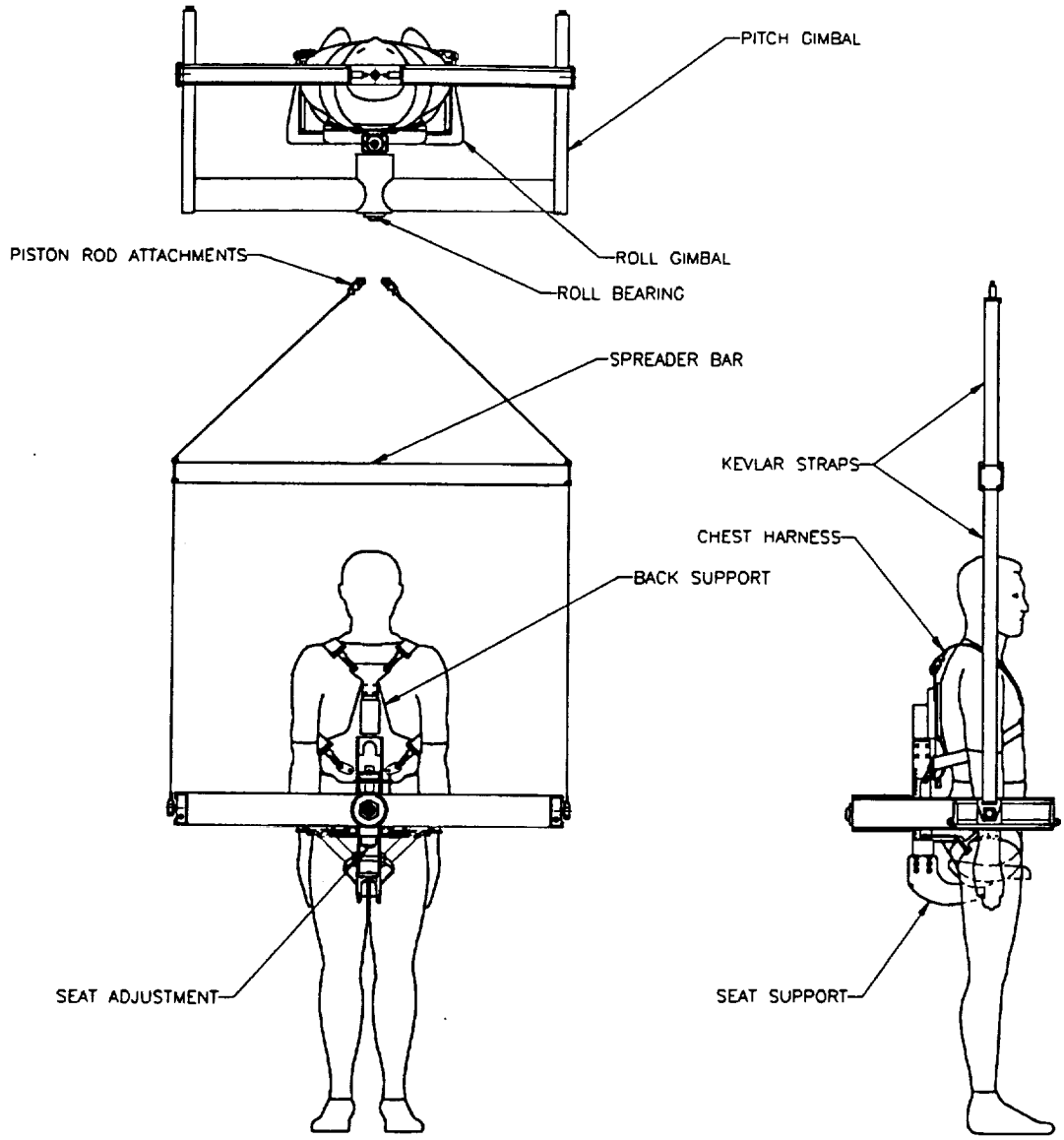

Figure 1(b). Gimbal support assembly.

(Illustration by Ray, adapted from NASA drawing SEY43116721, drawn by Brian Petty of the Johnson Engineering Corporation.)

2.2 Vertical Servo Flow System Description

Maintaining stability in pneumatic systems is a problem when designing closed loop pressure and flow controls. In transmissions of compressed air, harmonic oscillations or whistles can be generated given certain flow conditions coupled with changing line diameters, nozzles, and orifice restrictions. Such conditions are prevalent in the vertical servo flow control system, which is shown schematically in Figure 2. According to Burrows [3], "The main goal in designing a control system is to achieve adequate dynamic performance without the system becoming unstable." One of the design goals in developing a stable control system for the vertical servo is to determine the best combinations of supply pressure and flapper-nozzle control valve gap settings that result in stable performance of the two-stage mechanical amplification feedback of the Pogo vertical servo.

The Pogo vertical servo is a pressure and flow regulating device in which the amplification is error actuated. To be operated properly, the vertical servo needs to be a fast responding regulator, where the desired lift force from the piston/cylinder lifting actuator of Figure 1(a) is maintained constantly for a continuously varying input load at the end of the actuator.

The first step in developing a stable operating control system is to define the system. A control block diagram of the vertical servo flow control system is shown in Figure 3.

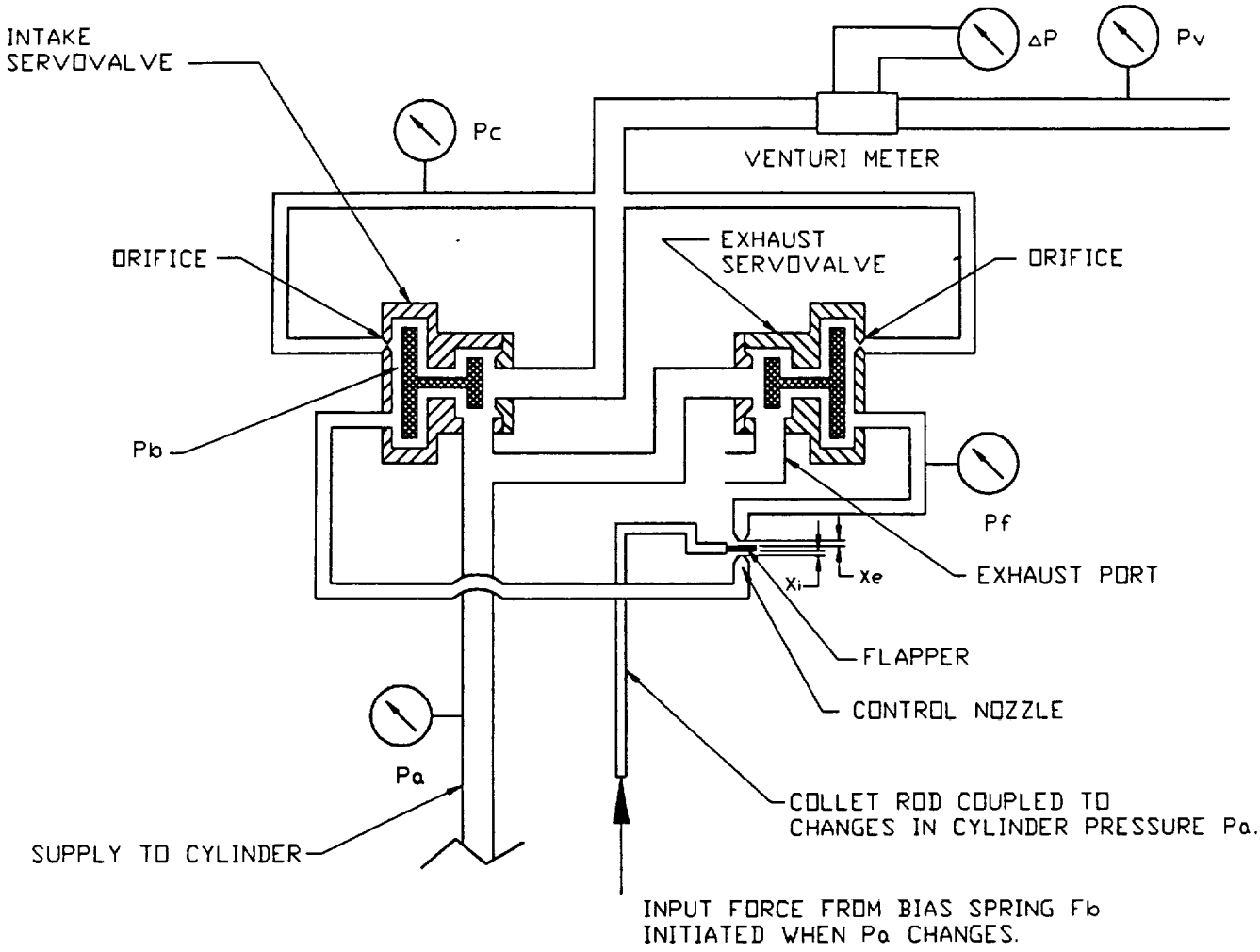

Figure 2. Vertical servo flow control system description.

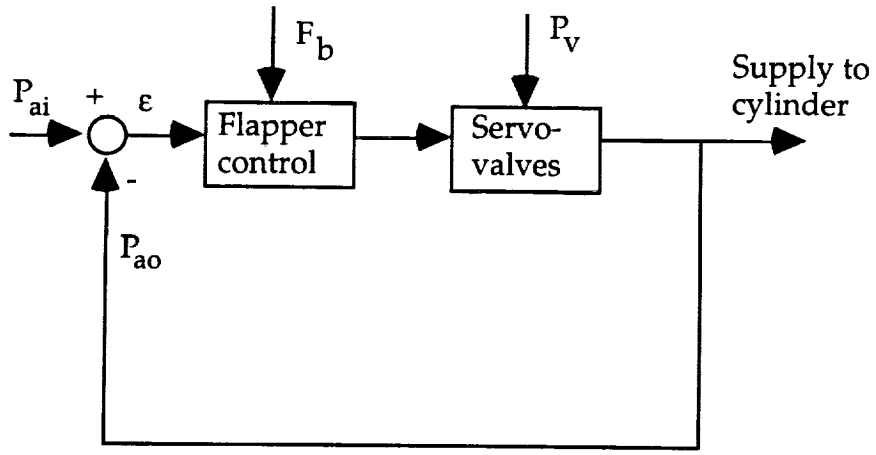

P_{ai} : Input lifting pressure to the cylinder.

P_{ao} : Instantaneous output to the cylinder.

ε : Error signal.

F_b : Bias spring input force which deflects the flapper.

P_v : Pressure supply to vertical servo.

Figure 3. Control block diagram for the two-stage vertical servo amplifier.

Figure 3 shows that the first stage of the vertical servo consists of the flapper-nozzle control valve, and that the second stage consists of the intake and exhaust servovalves. An instantaneous change in pressure P_{ao} in the cylinder, due to subject motion, is compared to the required input lifting pressure P_{ai} for constant partial gravity simulation. The result of this comparison is the error signal ε. The error is amplified by the flapper-nozzle control valve element F_b, which represents the influence of the bias spring force of the vertical servo shown in Figure 1(a). The flapper-nozzle controller in turn affects the back pressure Pb in the intake and exhaust servovalves, as seen in Figure 2. The back pressure Pb is considerably less than the control pressure Pc, due to the orifice restriction at the inlet to each servovalve control chamber. The servovalves act as a second

stage pressure regulating element, which further amplifies the error signal and supplies the required pressure change to the lifting cylinder to reduce the difference between P_{ai} and P_{ao}.

The flow control diagram in Figure 2 shows that the vertical servo acts basically as a two-way flow and pressure regulator. The main supply of air flow enters the intake of the valve chamber of the intake servovalve and is diverted in two different directions. One direction is the inlet to the lifting cylinder, and the other direction is the inlet to the exhaust servovalve. The amount of air flow going to either the cylinder or the exhaust is proportional to the back pressure Pb, which varies according to the position of the flapper between the control nozzles. The error signal ε is directly proportional to the position of the flapper between the control nozzles.

3.0 Test Objectives

The objectives of the tests on the Pogo vertical servo are accomplished in two parts. Part I is a static test dedicated to defining the pressure and flow characteristics of the vertical servo flapper control valve. The change in pressure in the lines connecting the intake and exhaust servovalves to the control nozzles is measured versus the gap between the flapper and the nozzle. Changes in volume flow rate through the vertical servo using a calibrated Venturi meter are also recorded. These pressure and flow readings are repeated at various inlet supply pressures P_V, which would be required to provide lift for subjects of various weights.

The objective of Part II of the tests is to determine the dynamic accuracy of the simulator by measuring force versus time data from the Pogo load cell and a load cell which measures foot/ground reaction forces. These data are collected with human test subjects performing walking and running exercises at gravity levels of one g, 0.95g, 3/8g, and 1/6g. A profile of the test subjects is given in Table 1. These empirical data will be analyzed and compared to results obtained by alternate partial gravity simulation methods.

Table 1. Profile of the Test Subjects Participating in the Pogo Tests

Test Subject	Age (years)	Weight (lb.)	Height (in.)	Gender
DN	29	110	64	Female
ML	31	158	71	Male
BP	32	170	70	Male
DR	28	176	73	Male

The configuration and test apparatus for both Parts I and II of the Pogo tests are shown in Figure 4. The instrumentation for Part I is as follows:

- A set of go/no-go feeler gauges to measure the gap in inches between the control flapper and the nozzles.

- Two pressure transducers to measure the control pressure to each servovalve Pc and the pressure in the line to the flapper valve Pf.

- A Venturi meter coupled with a strain gauge differential pressure transducer to measure the volume flow rate Q in scfm through the vertical servo. Venturi meter calibration is obtained from the NASA JSC Calibration and Standards Laboratory.

The instrumentation for Part II of the tests is as follows:

- A load cell connected to the end of the actuator piston rod for force measurements.

- A treadmill with load cells in the platform to collect foot force data from human locomotion inputs.

- All the test instrumentation is connected to the data acquisition system, which consists of the National Instrument SCXI-1120 signal conditioning module and Lab-PC analog to digital conversion card in an NEC 386/20 PC (personal computer). The National Instrument NI-DAQ software package is used for viewing and recording the real-time responses of the load cells.

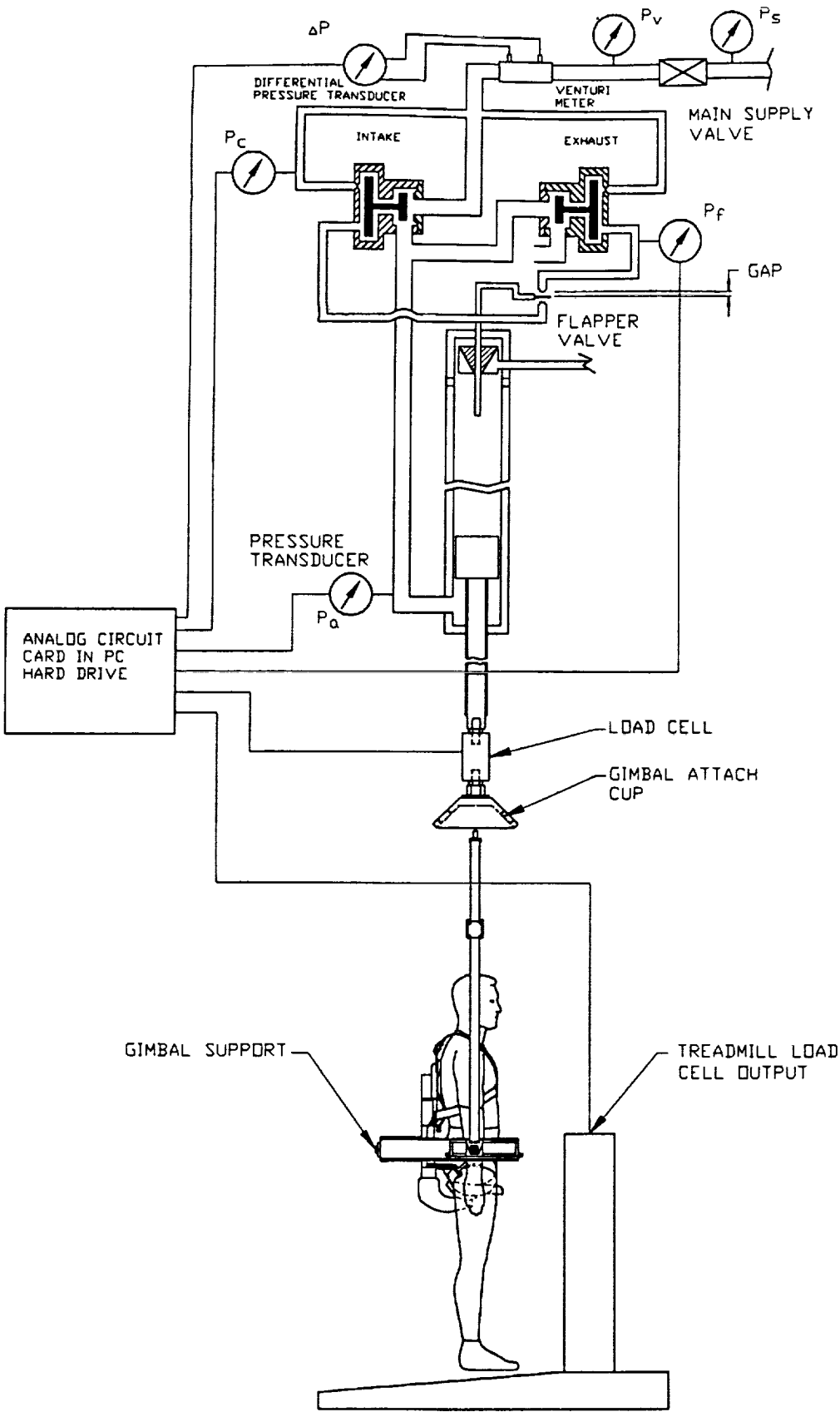

Figure 4. Pogo test configuration.

4.0 Flapper Control Valve Pressure and Flow Curves

Figure 5 shows the static equilibrium pressure curves for the flapper-nozzle control valve sensor. The figure depicts values of Pf (Pf is the pressure in the line connected to the control chamber of the exhaust servovalve shown in Figure 4) as a function of the gap or distance between the flapper and the nozzle. The static pressure curves are recorded at various supply pressures to the vertical servo, which is depicted as P_v. The values chosen for P_v vary between 25 and 50 psig. These values are chosen for P_v because they represent the range of pressures required to lift the various test subjects at the required simulated gravity levels.

Figure 6 shows the flow rate Q through the vertical servo in scfm as a function of the gap between the flapper and the control nozzle. The flow rates are also measured at various supply pressures P_v. For each value of Q for a given P_v and gap setting in Figure 6, there is a corresponding value of Pf in Figure 5. Thus, each gap setting for a particular value of P_v has a distinct value for Pf and Q.

The pressure versus gap curves in Figure 5 show that Pf decreases rapidly as the gap increases from 0.002 to 0.004 in. for all values of P_v. Then the pressure remains relatively constant to a gap of 0.006 in. It decreases again to a gap of 0.008 in. Data are not collected for gap values greater that 0.008 in., since an increase in the gap beyond this value creates excessive noise levels due to the exhausting air. Figure 6 shows the changes in volume flow rate to be fairly constant from a gap of 0.000 to 0.003 in. for all values of P_v, but then the volume flow rate increases rapidly from a gap of 0.003 to 0.008 in.

The information given in Figures 5 and 6 is used as a tool to develop the correct gap settings of the flapper-nozzle control valve. The problem in determining the proper gap setting for the control flapper deals with providing the proper pressure change in Pf, for a given change in gap, while maintaining a certain flow rate through the servo to make up for

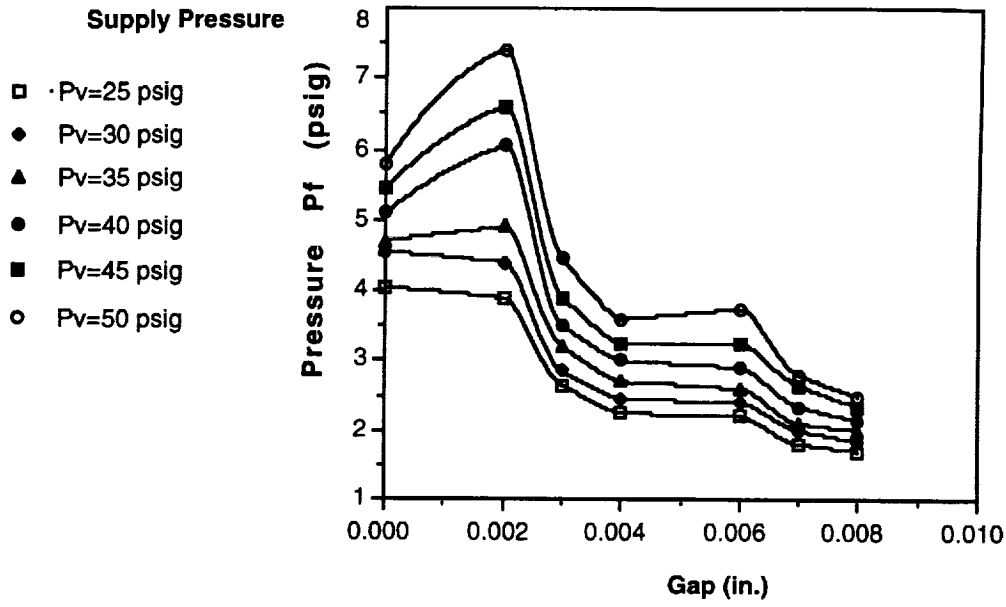

Figure 5. Pressure characteristic curves for the flapper-nozzle control valve sensor.

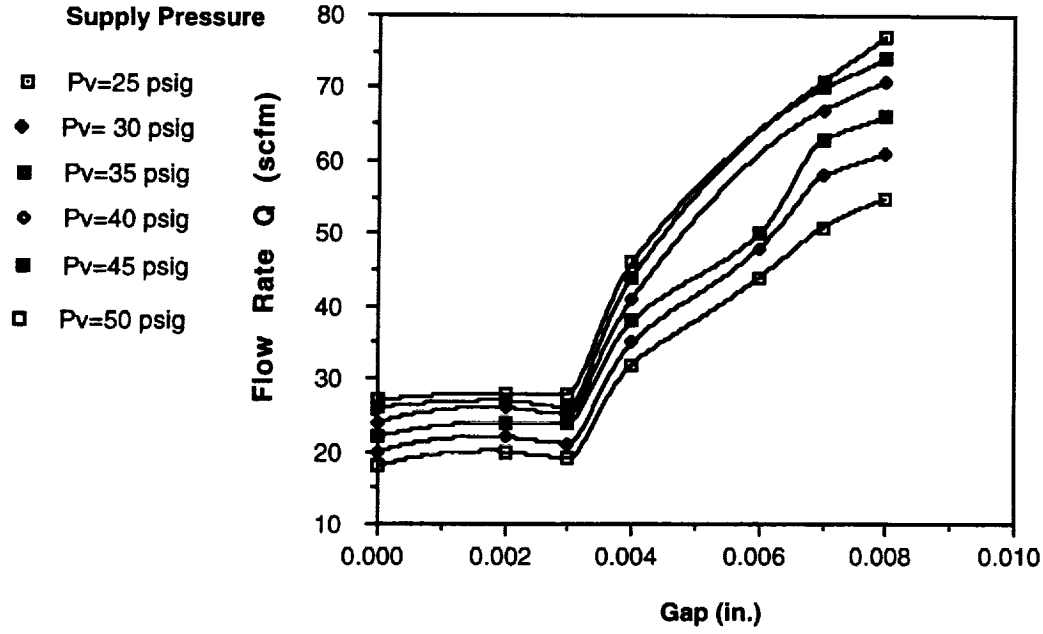

Figure 6. Volume flow rate through the vertical servo as a function of the flapper-nozzle gap at different supply pressures P_v.

the movement of the piston rod in the actuator cylinder. After interpreting the data in Figures 5 and 6, the gap x_e (from Figure 2) is set at 0.004 in. and x_i is set at 0.008 in.

5.0 Simulator Response to Human Locomotion

The following results show the Pogo system response to human locomotion at various gravity levels and the mean stride frequencies and mean peak foot forces of the test subjects at these gravity levels. For the tests, the DelMar treadmill (Figure 4) is used on a level surface. The treadmill has a variable speed from 0 to 10 mph. Speeds of 2 mph and 6.5 mph are used for the tests, where 2 mph is considered a walking speed and 6.5 mph is considered a running speed.

Walking and running exercises are performed on the treadmill at gravity levels of 3/8g (martian gravity), 1/6g (lunar gravity), and one g (Earth gravity). Figures 7(a) through 7(p) show the results of the load cell time traces for each of the four test subjects who were walking and running at 1/6g and 3/8g using Pogo. Information on each test subject can be found in Table 1.

Ideally, the force traces in Figures 7(a) through 7(p), which are designated "Pogo Lift Force," should be constant over time and coincide with the dashed line designated "Ref. Lift Force," which represents the force to be maintained to provide constant partial gravity simulation. The force trace designated "Tread Force" represents the foot reaction forces measured by the load cells in the treadmill platform.

The force versus time traces of Figures 7(a) through 7(p) show that the Pogo lift force deviates from the constant reference lift force for each case. For some cases, the Pogo lift force is fairly steady and consistent over the given time intervals, which can include as many as 12 steps. For other cases, the Pogo lift force deviates frequently and is discontinuous over the time intervals. For instance, Figure 7(b) shows that, for test subject DN, the required lifting force is 158 lbf and the variation in Pogo lift force ranges from 152 to 158 lbf. For this case, the percent error, which is presented here as the percentage of the ratio of the maximum deviation from the reference lifting force to the reference

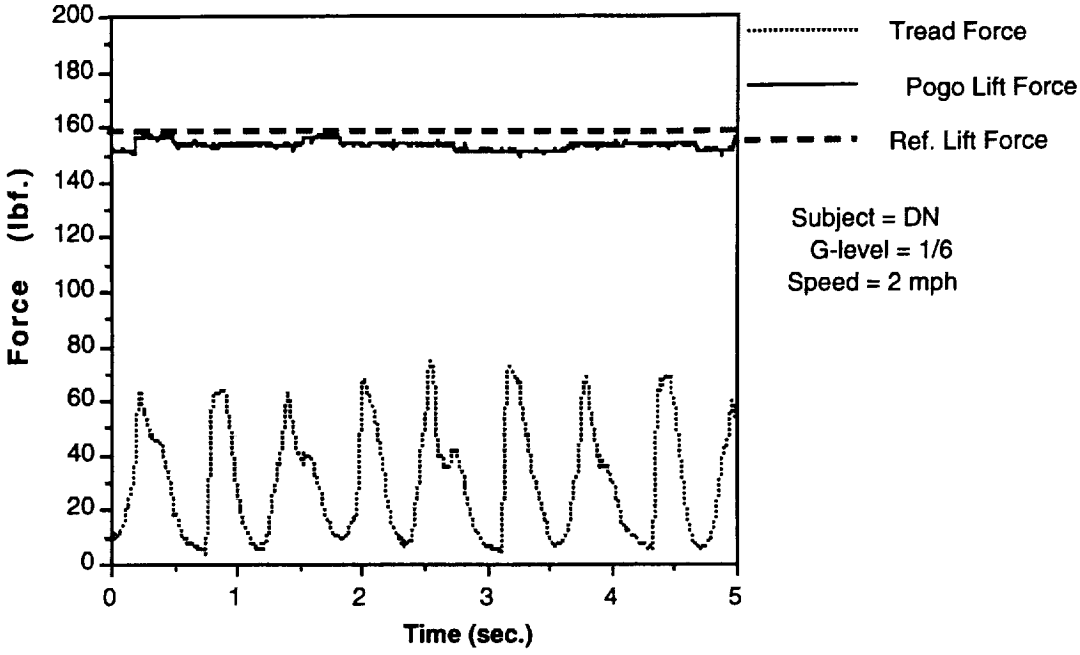

Figure 7(a). Load cell force traces from test subject DN walking at 2 mph at 1/6g.

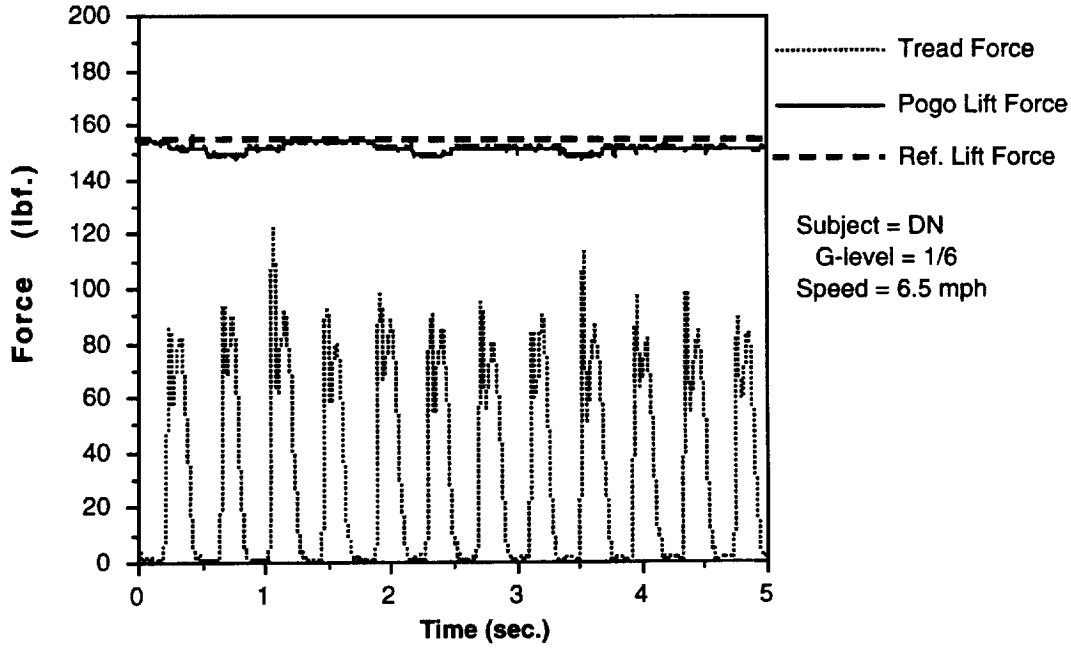

Figure 7(b). Load cell force traces from test subject DN running at 6.5 mph at 1/6g.

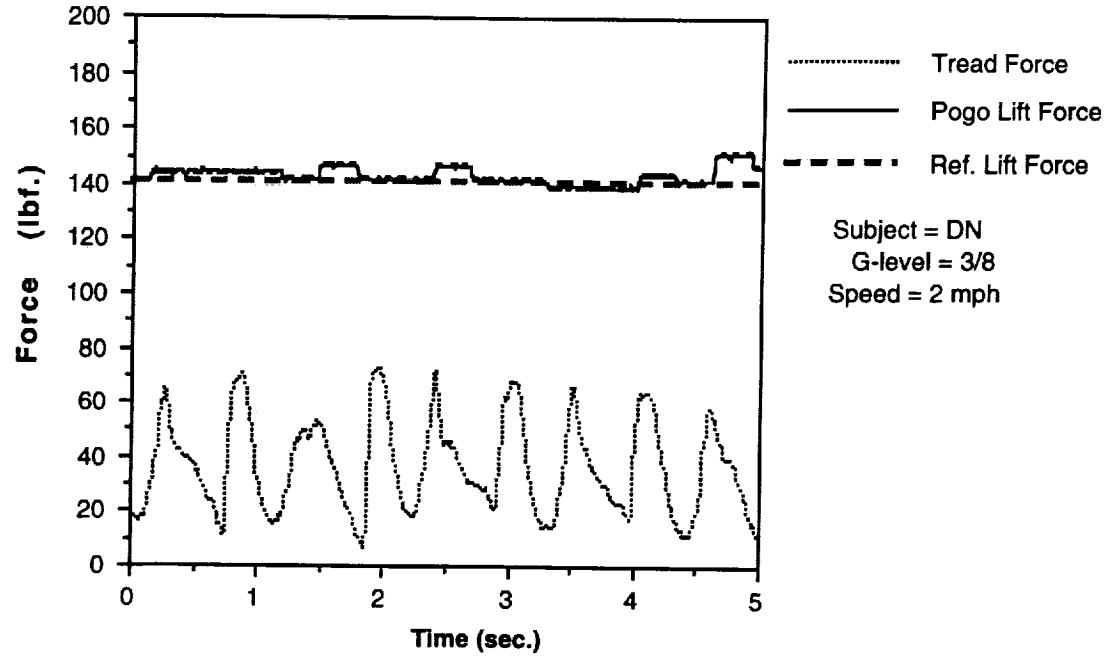

Figure 7(c). Load cell force traces from test subject DN walking at 2 mph at 3/8g.

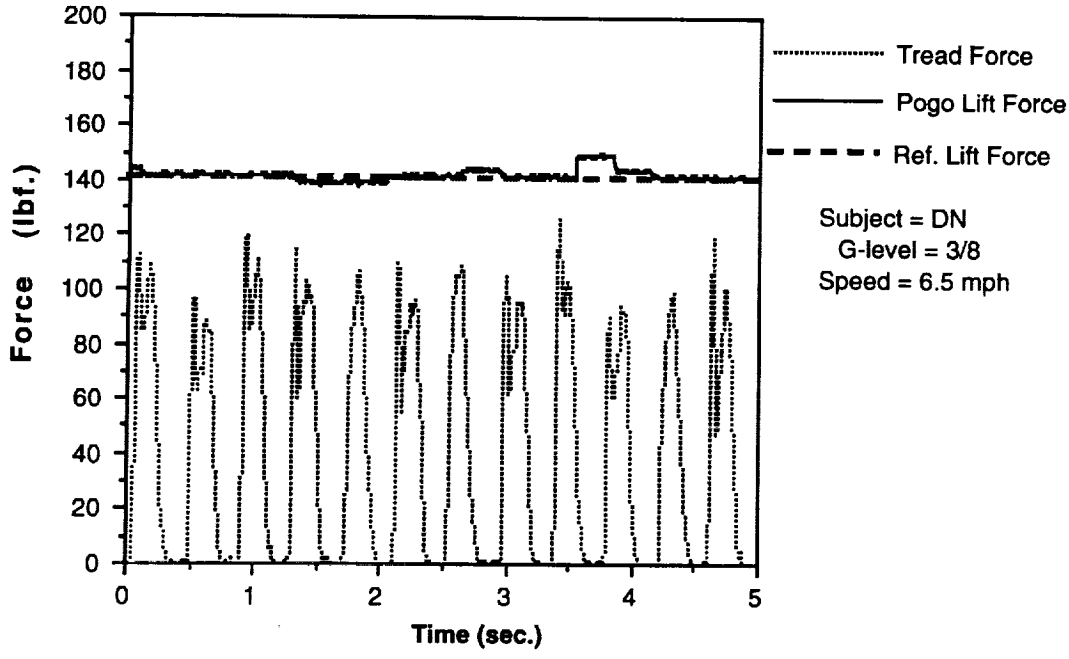

Figure 7(d). Load cell force traces from test subject DN running at 6.5 mph at 3/8g.

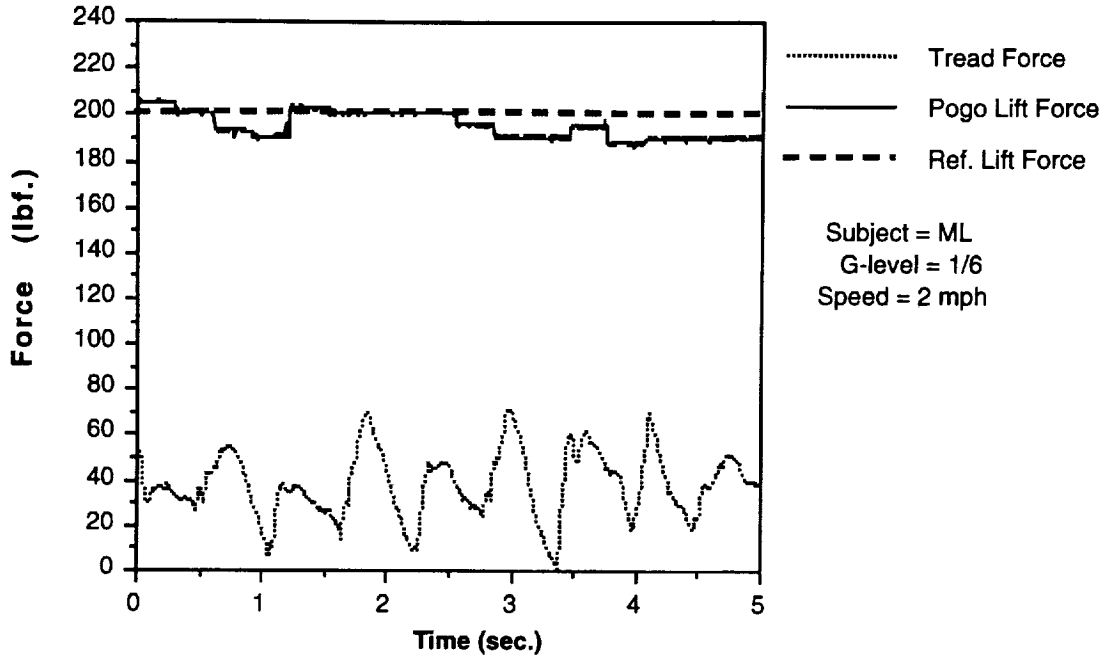

Figure 7(e). Load cell force traces from test subject ML walking at 2 mph at 1/6g.

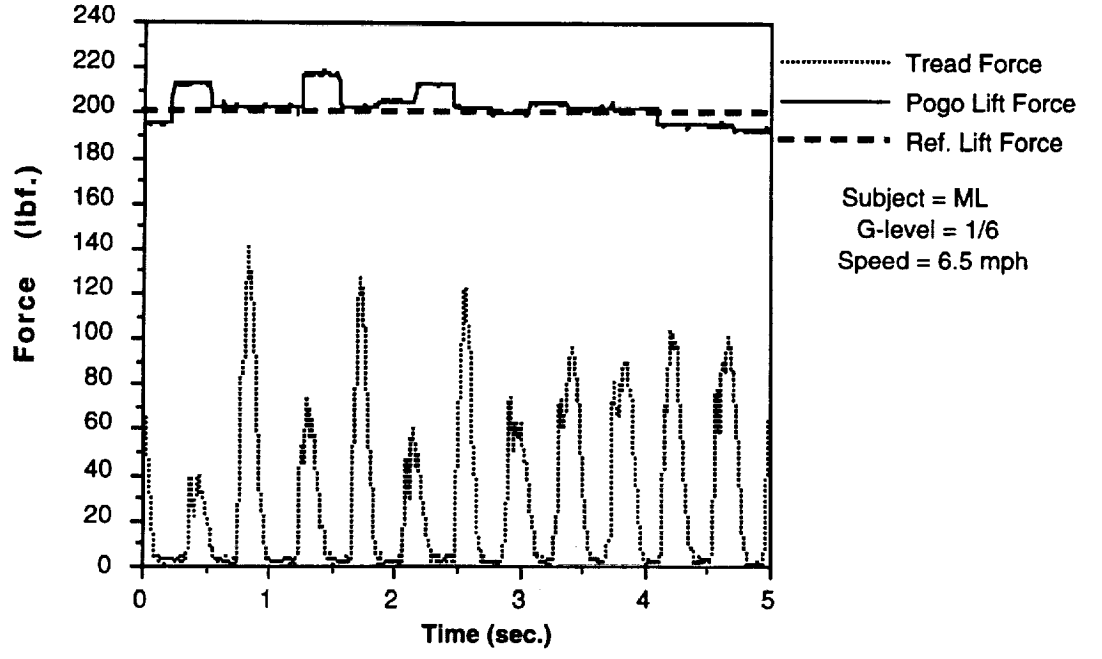

Figure 7(f). Load cell force traces from test subject ML running at 6.5 mph at 1/6g.

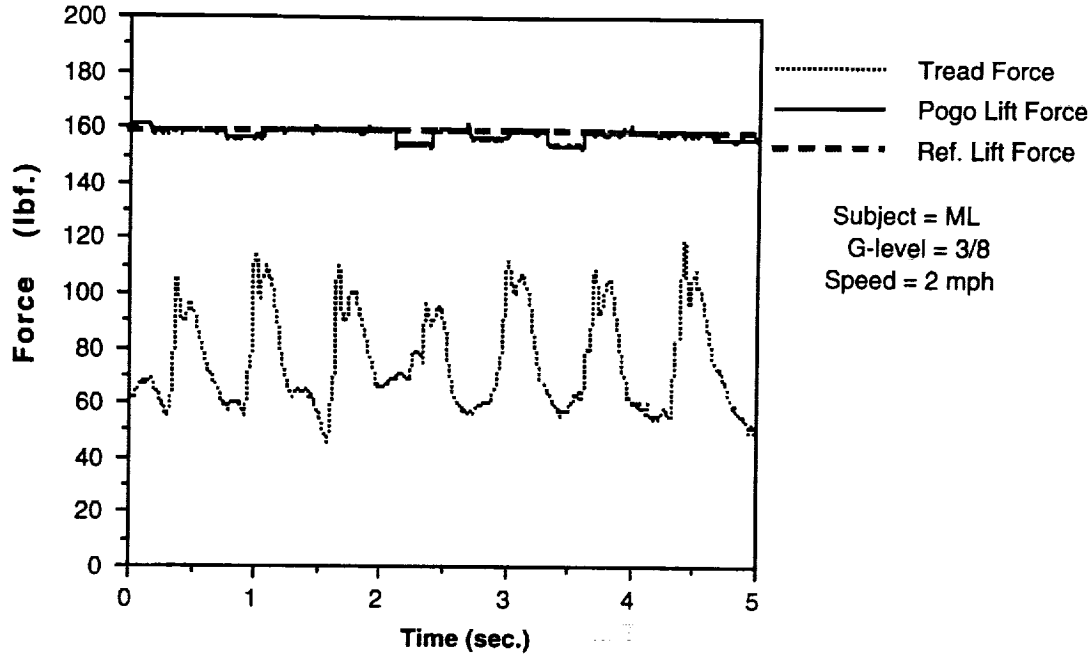

Figure 7(g). Load cell force traces from test subject ML walking at 2 mph at 3/8g.

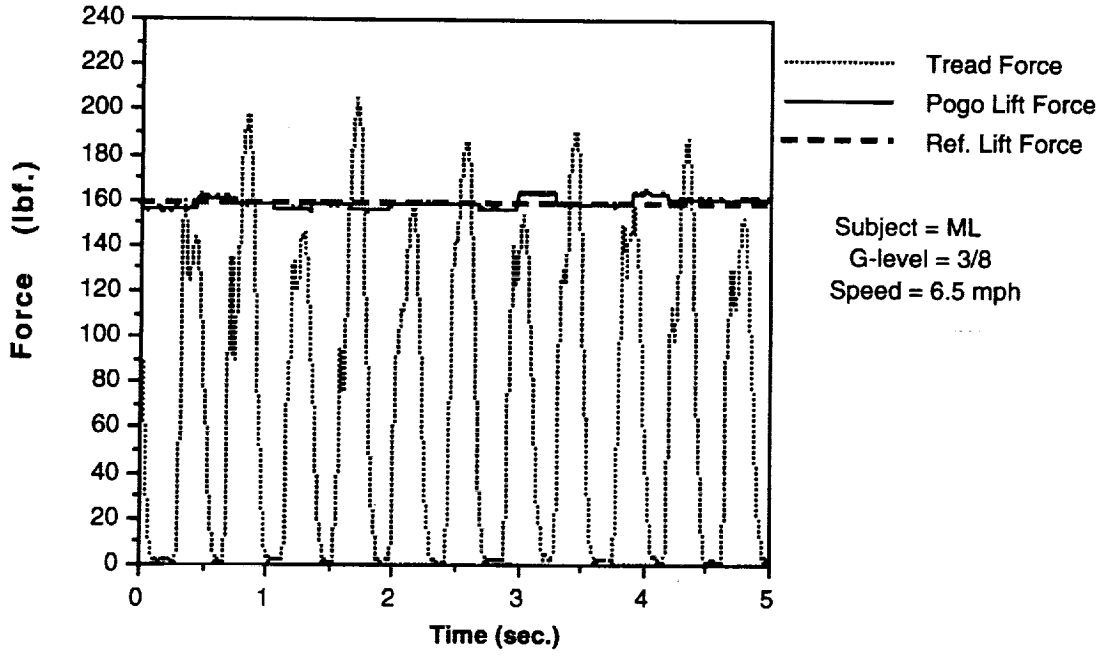

Figure 7(h). Load cell force traces from test subject ML running at 6.5 mph at 3/8g.

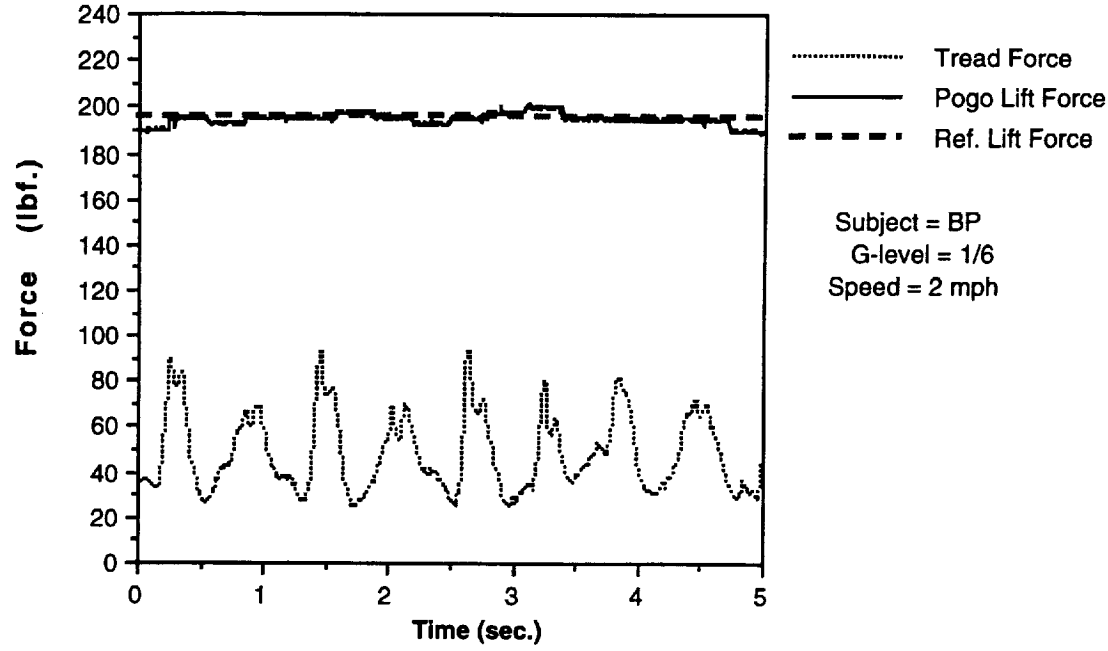

Figure 7(i). Load cell force traces from test subject BP walking at 2 mph at 1/6g.

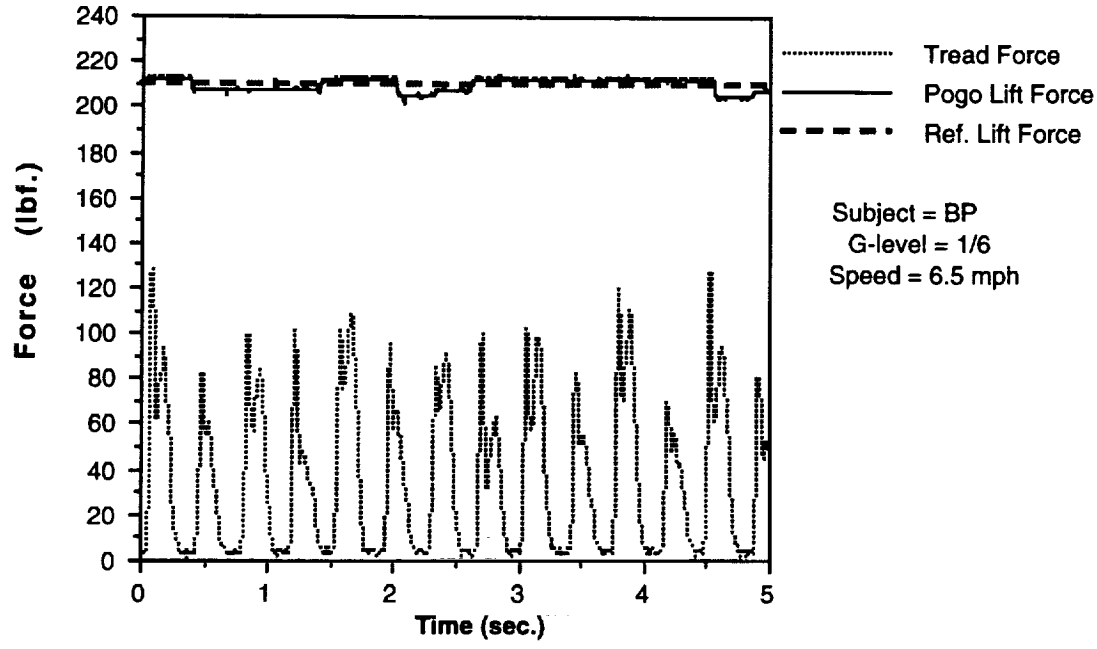

Figure 7(j). Load cell force traces from test subject BP running at 6.5 mph at 1/6g.

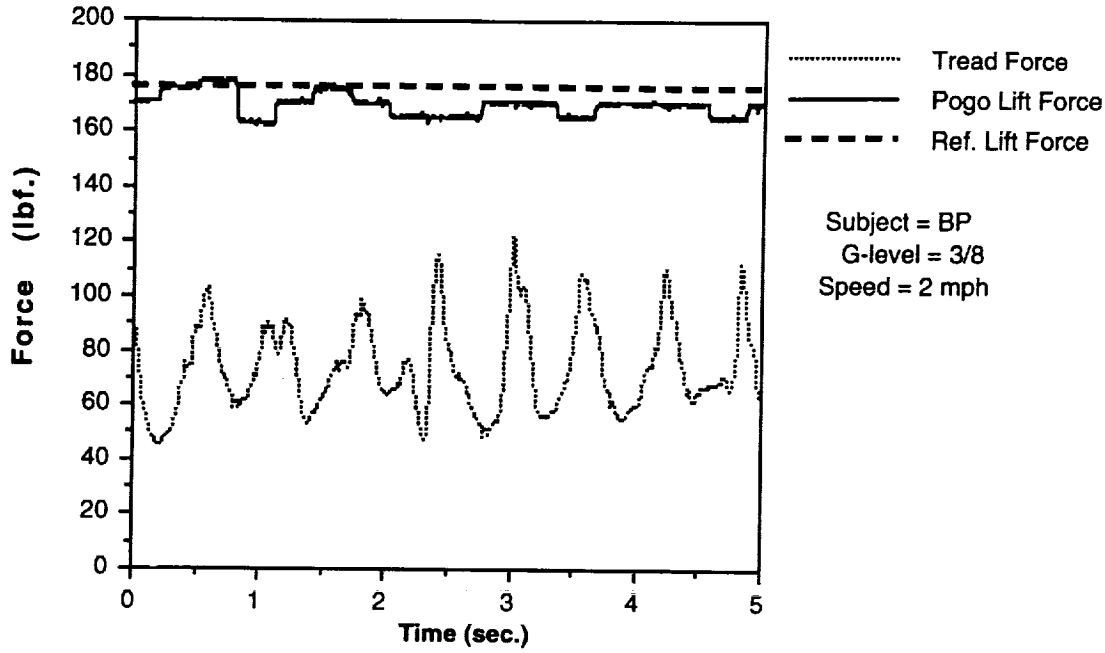

Figure 7(k). Load cell force traces from test subject BP walking at 2 mph at 3/8g.

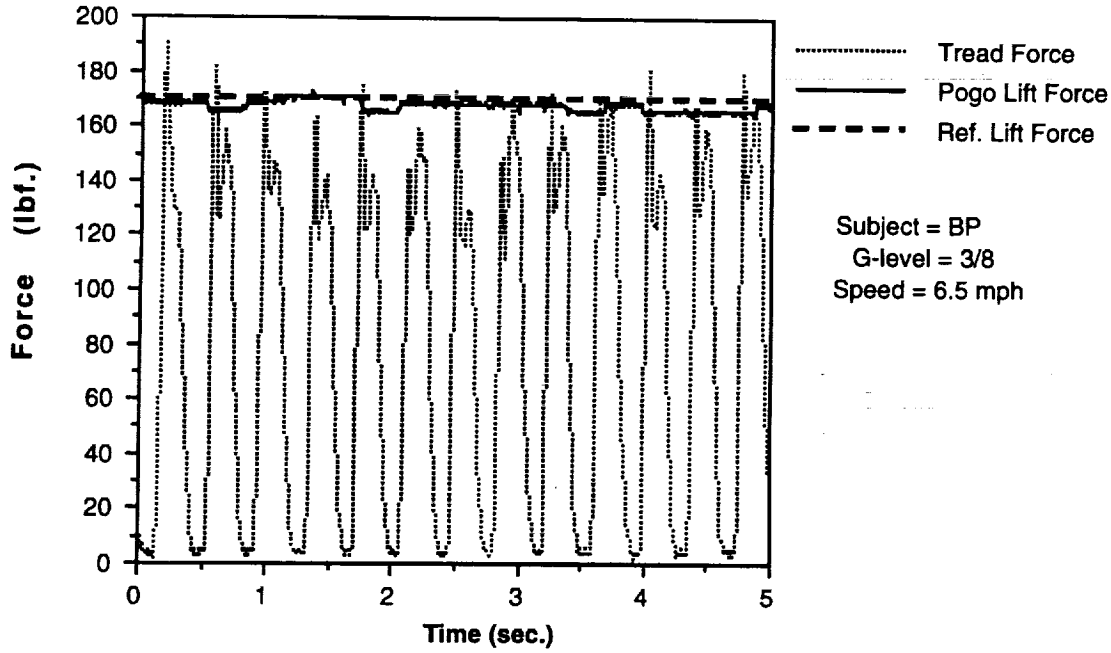

Figure 7(l). Load cell force traces from test subject BP running at 6.5 mph at 3/8g.

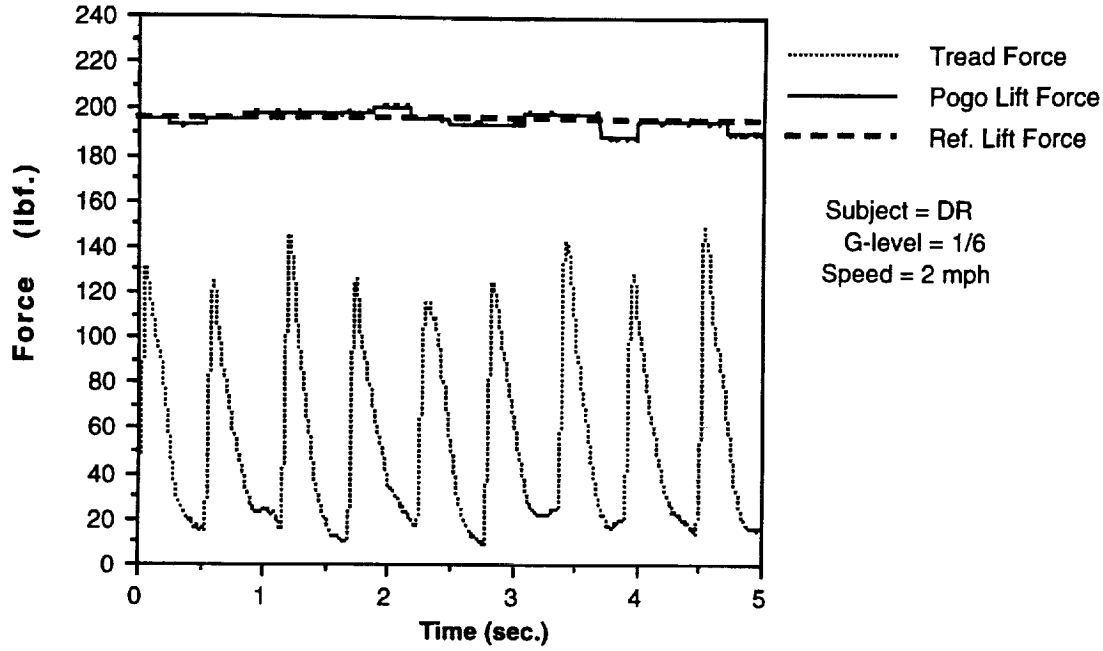

Figure 7(m). Load cell force traces from test subject DR walking at 2 mph at 1/6g.

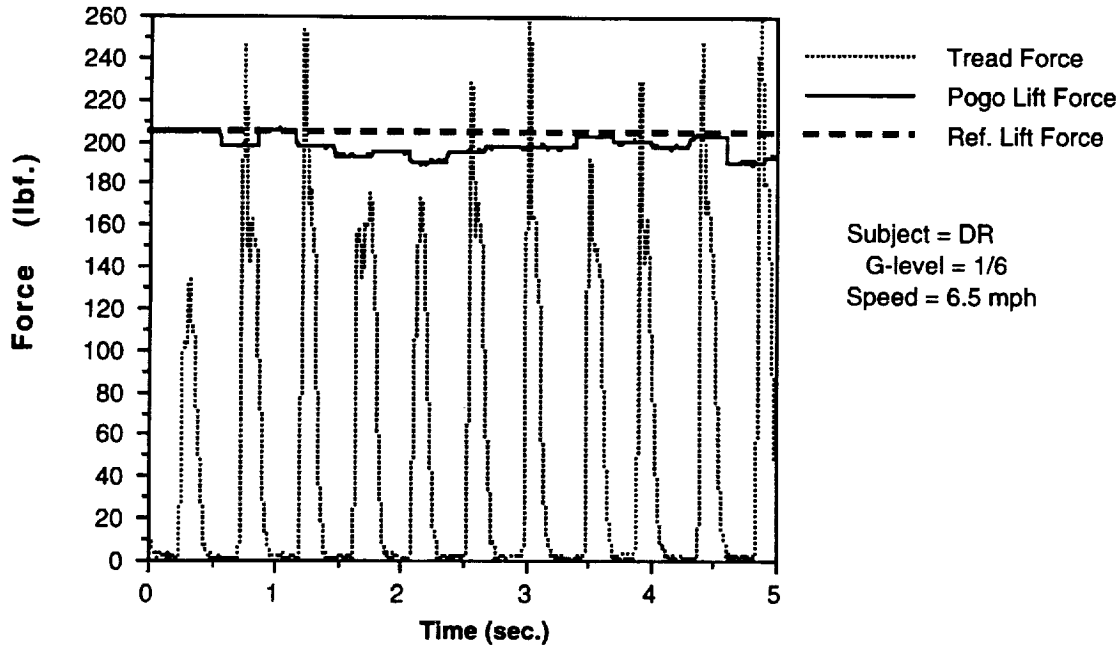

Figure 7(n). Local cell force traces from test subject DR running at 6.5 mph at 1/6g.

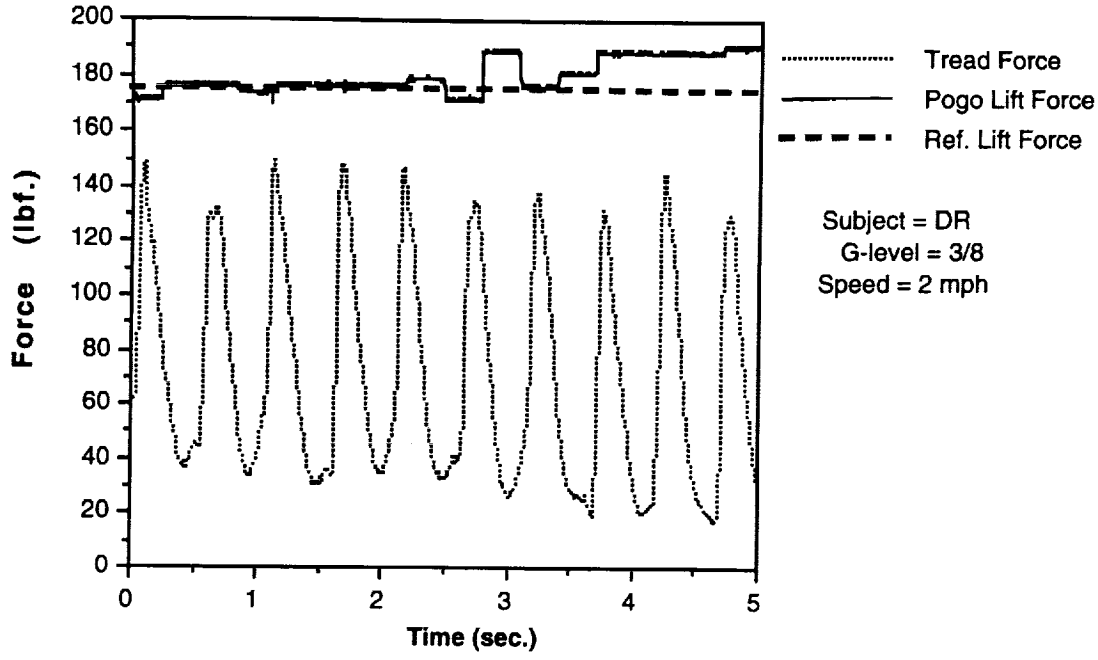

Figure 7(o). Local cell force traces from test subject DR walking at 2 mph at 3/8g.

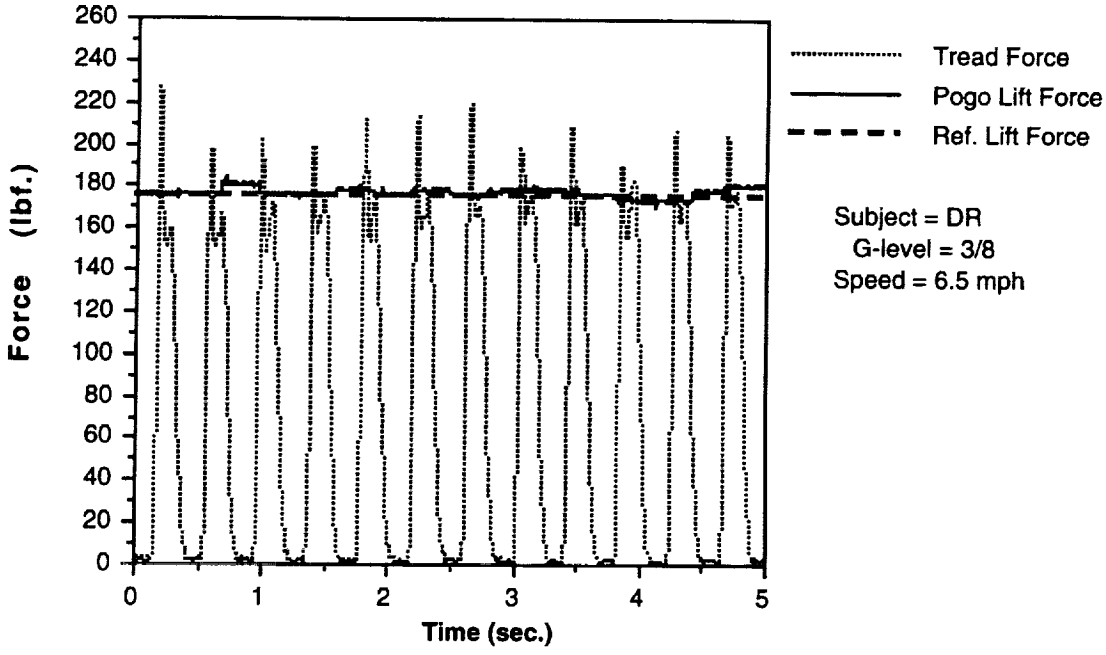

Figure 7(p). Load cell force traces from test subject DR running at 6.5 mph at 3/8g.

lifting force, is (158 lbf-152 lbf)/158 lbf or 3.8%. Figure 7(f) shows that, for test subject ML, the required reference lifting force is 200 lbf, and the variation in the Pogo lift force ranges from 190 to 220 lbf. The percent error for this case is 20 lbf/200 lbf or 10%. The percent error in maintaining partial gravity simulation for each test case is presented in Table 2.

The discontinuities in the Pogo lift force for each case are not expected because the flow through the vertical servo is a continuous process. However, discontinuities could be caused by a number of factors. The supply pressure available from the facility is not constant, and demands placed on the compressed air supply from other users can cause pressure fluctuations. The poppets in the servovalves have precision clearances to provide for air-bearing surfaces. These surfaces can collect dirt and oil from the air supply and cause the poppets to stick. If the poppets are not moving freely in a continuous manner, the output to the lifting cylinder will not be continuous. Finally, the human locomotion inputs cause lateral motions to be imparted to the lifting cylinder. These lateral motions can cause deviations in the Pogo load cell readings because the load cell is designed and calibrated to record pure tension forces. In some cases (Figures 7(f) and 7(n)), there are noticeable discontinuities in the Pogo lift force that correspond with noticeable differences in the peaks between simultaneous tread force traces. In other cases (Figures 7(d) and 7(j)), the Pogo lift force traces are fairly consistent when the peaks in simultaneous tread force traces are also fairly steady and consistent.

Figures 8 and 9 present the mean results, with the standard deviations from the mean, of the biomechanic data for the four test subjects who are walking and running at different gravity levels. Figure 8 shows the mean stride frequency in strides/minute versus gravity level. Figure 9 shows mean dimensionless peak force versus gravity level. Stride frequency is calculated from tread force traces using the time it takes to put one foot down, pick it up, and put it down again, which represents one stride period. Dimensionless

Table 2. Percent Error in Maintaining Partial Gravity Lifting Force

(Percent error is found using the maximum deviation from the reference lifting force.)

Subject	G-level speed	Percent error
DN	1/6g 2 mph	5.0
DN	1/6g 6.5 mph	3.8
DN	3/8g 2 mph	7.1
DN	3/8g 6.5 mph	6.4
ML	1/6g 2 mph	6.0
ML	1/6g 6.5 mph	10.0
ML	3/8g 2 mph	3.1
ML	3/8g 6.5 mph	3.1
BP	1/6g 2 mph	2.5
BP	1/6g 6.5 mph	2.4
BP	3/8g 2 mph	9.1
BP	3/8g 6.5 mph	2.9
DR	1/6g 2 mph	4.0
DR	1/6g 6.5 mph	7.3
DR	3/8g 2 mph	6.7
DR	3/8g 6.5 mph	2.2

peak force is defined as measured peak force divided by the subject's weight at one g. Both Figures 8 and 9 contain data collected at gravity levels of 1/6g, 3/8g, 0.95g, and one g where the 0.95g level represents human locomotion while connected to the gimbal support assembly. The 0.95g data are collected to determine how the gimbal support

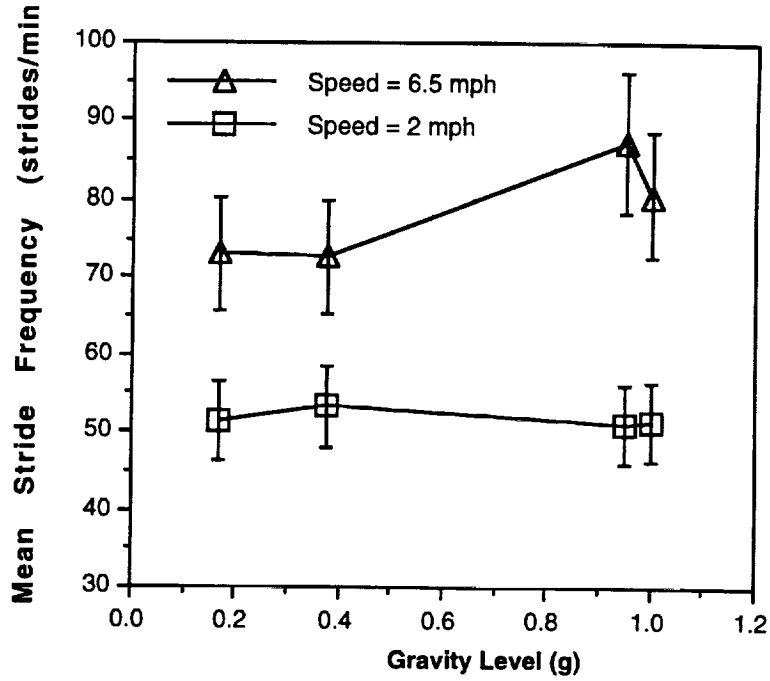

Figure 8. Mean stride frequency with standard deviations from the mean versus gravity level for four test subjects.

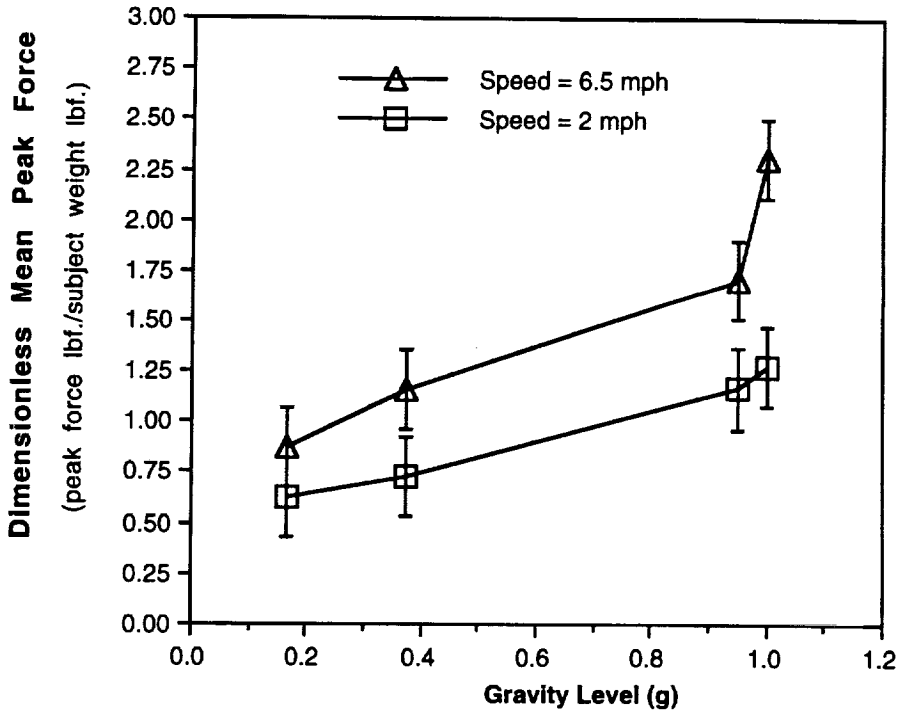

Figure 9. Dimensionless mean peak force with standard deviations from the mean versus gravity level for four test subjects.

affects human locomotion performance by comparing the 0.95g data to the one-g data, where at one g the test subjects are not supported by the gimbal.

Figures 8 and 9 reveal that values for mean stride frequency and mean peak force vary from the expected trend for running speeds at 0.95g, which indicates that the support gimbal reduces human locomotion performance by increasing stride frequency and decreasing peak force. The data shown at 0.95g are expected because test subjects commented that the gimbal limited their leg motion while running at 0.95g, which indicates that, as the normal stride period decreases, stride frequency increases. The reduced stride period also indicates less aerial time for each step, which reduces the potential energy of each step and the mean peak force.

The data plotted in Figures 8 and 9 show that the support gimbal definitely adversely affects the expected stride frequency and peak force for the running speed of 6.5 mph at 0.95g. Now the results of the data in Figures 8 and 9 are compared to alternate partial gravity simulation methods to determine the effects of the gimbal on stride frequency and peak force at 1/6g and 3/8g. The results of Figures 8 and 9 are compared to the results from Newman [4] using underwater immersion to simulate partial gravity, and with the results from Hewes [5] using an inclined plane partial gravity simulator. Table 3 presents a comparison of the mean stride frequency and dimensionless peak force results based on percent reductions from the one-g data.

A comparison of results shown in Table 3 reveals some distinct discrepancies and some similarities between the different methods of partial gravity simulation. For walking speeds at 1/6g, the results for percent reduction in stride frequency are very different. For Pogo, there is no distinguishable difference between stride frequencies for the walking speed at different gravity levels; therefore, a 0% reduction is listed. Underwater immersion results from Newman [4] show a 26% reduction in stride frequency at 1.1 mph as opposed to a 15% reduction from Hewes [5] at 2 mph using an inclined plane.

Table 3. Percent Reduction of the Pogo Mean Stride Frequency and Dimensionless Peak Force Results versus Alternate Partial Gravity Simulation Methods

Source of results	Gravity level (g)	Speed mph	Reduction in stride freq. (%)	Reduction in peak force (%)
Ray	1/6	2	0	50
Newman [4]	1/6	1.1	26	76
Hewes [5]	1/6	2	15	N/A
Ray	1/6	6.5	12	62
Newman [4]	1/6	5.13	47	76
Hewes [5]	1/6	6.5	44	N/A
Ray	3/8	2	0	44
Newman [4]	3/8	1.1	21	68
Ray	3/8	6.5	12	51
Newman [4]	3/8	5.13	36	52

The data for percent reduction in peak force are similar for Pogo and the underwater immersion results, but peak force data from Hewes is not available for comparison. For running speeds at 1/6g, Pogo results show a 62% reduction in peak force as compared to a 76% reduction from underwater immersion. For running speeds at 3/8g, Pogo shows a 51% reduction in peak force, which compares very well with a 52% reduction from underwater immersion.

A comparison of the results in Table 3 definitely reveals that the percent reduction in stride frequency for Pogo is less than expected. The cause of the lack of stride frequency reduction is attributed to the effects of the gimbal support seat on leg motion. As described

previously for the 0.95g level in Figure 8, the stride frequency is greater than expected due to the restriction of the gimbal support seat. A comparison of the results in Table 3 indicates that the gimbal support seat also causes an increase in stride frequency at lower gravity levels. Therefore, the data collection process used to create Figures 8 and 9 and the comparison of results in Table 3 provide a method to test future modifications to the gimbal support which would allow for increased leg motion.

6.0 Summary and Conclusions

The results of the pressure and flow curves are very useful tools in developing proper adjustments to the flapper-nozzle control valve before proceeding to conduct tests or training exercises at partial gravity levels. Results of the Pogo lifting response to human locomotion are very encouraging. The load cell force traces in Figures 7(a) through 7(p) show that Pogo responds favorably to human locomotion inputs. Test results in Table 2 show that the Pogo performance, in the worse case, deviates a maximum of 10% from the required constant lift force or constant partial gravity simulation. These results also show that the error range in Pogo constant lift capabilities ranges from 10 to 2.2% depending on the test subject, the type of locomotion, and the simulated gravity level. Therefore, the Pogo vertical servo assembly is capable of providing partial gravity simulation within acceptable error ranges.

A comparison of the results of stride frequency data from the Pogo simulator with alternate methods of partial gravity simulation reveals significant differences. These differences are attributed to restrictions imposed by the gimbal support on normal leg motion. The data collected and the procedures established, however, allow for testing of future modifications and changes to the gimbal to reduce these restrictions.

In conclusion, the advantages and disadvantages and the future of the Pogo pneumatic actuator with closed loop mechanical amplification are presented. The major advantage of the Pogo simulator is that there is no time limit on the duration of simulation. During recent tests conducted on Pogo, former astronaut John Young commented that he ran 13.6 miles on the simulator when it was operational during the Apollo Program. Another advantage is that the percent error obtained in constant lift from the vertical servo is as low as 2.2% in some cases. Current disadvantages in using Pogo pertain to the gimbal support assembly. The gimbal support seat is uncomfortable and restricts normal stride

motions. Another disadvantage is that arms and legs do not experience partial gravity weight alleviation. Finally, the data presented will definitely be used in the future to support partial gravity and microgravity training and physiological studies for NASA manned missions in orbiting Space Stations or lunar and Mars missions. The research conducted can be used to develop higher fidelity simulators with additional degrees-of-freedom and to develop heavy lift simulators to provide partial gravity simulation for spacecraft and payloads of various sizes.

7.0 References

[1] A. G. Trader and H. I. Johnson. Pneumatic Amplifier Controls High Pressure Fluid Supply, NASA Tech Brief, Brief 71-10081, April 1971.

[2] D. M. Ray. Partial Gravity Simulation Development, JSC Research and Technology 1991 Annual Report, NASA Technical Memorandum 104747, Section II-51.

[3] C. R. Burrows. Fluid Power Mechanisms, 1st ed., London: Van Nostrand Reinhold Co., 1972.

[4] D. J. Newman. Human Locomotion in Simulated Partial Gravity, M.I.T., Doctoral dissertation, 1992.

[5] D. E. Hewes. Reduced Gravity Simulator for Studies of Man's Mobility in Space and on the Moon, *Human Factors*, Vol. 11, pp. 419-425, 1969.

REPORT DOCUMENTATION PAGE

Form Approved
OMB No. 0704-0188

1. AGENCY USE ONLY *(Leave blank)*	2. REPORT DATE	3. REPORT TYPE AND DATES COVERED
	June 1994	Technical Memorandum

4. TITLE AND SUBTITLE
Partial Gravity Simulation Using a Pneumatic Actuator with Closed Loop Mechanical Amplification

5. FUNDING NUMBERS

6. AUTHOR(S)

David M. Ray

7. PERFORMING ORGANIZATION NAME(S) AND ADDRESS(ES)

Flight Crew Support Division
Lyndon B. Johnson Space Center
Houston, TX 77058

8. PERFORMING ORGANIZATION REPORT NUMBER

S-772

9. SPONSORING / MONITORING AGENCY NAME(S) AND ADDRESS(ES)

National Aeronautics and Space Administration
Washington, D.C.

10. SPONSORING / MONITORING AGENCY REPORT NUMBER

NASA TM-104798

11. SUPPLEMENTARY NOTES

12a. DISTRIBUTION / AVAILABILITY STATEMENT

NASA Center for AeroSpace Information
800 Elkridge Landing Road
Linthicum Heights, MD 21090-2934
(301) 621-0390

Subject category: 14

12b. DISTRIBUTION CODE

13. ABSTRACT *(Maximum 200 words)*

To support future manned missions to the surface of the Moon and Mars or missions requiring manipulation of payloads and locomotion in space, a training device is required to simulate the conditions of both partial and microgravity as compared to the gravity on Earth. The focus of this paper is to present the development, construction, and testing of a partial gravity simulator which uses a pneumatic actuator with closed loop mechanical amplification.

The results of the testing show that this type of simulator maintains a constant partial gravity simulation with a variation of the simulated body force between 2.2% and 10%, depending on the type of locomotion inputs. The data collected using the simulator show that mean stride frequencies at running speeds at lunar and martian gravity levels are 12% less than those at Earth gravity. The data also show that foot ground reaction forces at lunar and martian gravity are, respectively, 62% and 51% less than those on Earth.

14. SUBJECT TERMS	15. NUMBER OF PAGES
Missions, Lunar and Martian; Microgravity; Partial Gravity Simulator; Mean Stride Frequencies; Foot Ground Reaction Forces	42
	16. PRICE CODE

17. SECURITY CLASSIFICATION OF REPORT	18. SECURITY CLASSIFICATION OF THIS PAGE	19. SECURITY CLASSIFICATION OF ABSTRACT	20. LIMITATION OF ABSTRACT
Unclassified	Unclassified	Unclassified	UL